A NEW STRUCTURE IN THE La-Li-Fe-O SYSTEM

F. ABBATTISTA, D. MAZZA and M. VALLINO

Dipartimento di Scienza dei Materiali e Ingegneria Chimica, Politecnico di Torino, Torino (Italy)

M. GAZZANO

Centro di Studio per la Fisica delle Macromolecole, Università di Bologna, Via Selmi 2, Bologna (Italy)

Summary

The single crystal structure determination of a new phase, belonging to the La-Li-Fe-O system, is reported (1456 measured reflections, $R_w = 0.020$, space group $P4/mbm$). This phase has the formula per unit cell $La_{24}Fe_6Li_{22}O_{56}$ with iron in its trivalent state. The preparative route is described, together with some equilibrium relationships with other phases, occurring in the same ternary system. The powder diffraction intensities, hkl and $d_{(hkl)}$, are also reported.

1. Introduction

The La-Li-Fe-O system has been investigated previously [1, 2] where we identified two new phases: $La_{1.75}Li_{0.75}Fe_{0.5}O_{3.92}$ (space group $I4/mmm$, K_2NiF_4 structure) and $La_{36}Li_{18}Fe_8O_{76}$ (space group $Im3m$, with a novel structure). In both these compounds, prepared in an oxidizing atmosphere ($p_{O_2} = 1$ and 0.21 atm respectively), iron possesses prevalently the oxidation number of 4+.

The lack of information about the existence of the Fe^{3+} containing member of the mixed oxide family with general formula $La_2Li_{0.5}M^{3+}_{0.5}O^*_4$ and K_2NiF_4-type structure, induced us to attempt its preparation under conditions appropriate for the prevention of formation of Fe^{4+} ions (*i.e.* reducing atmosphere of Ar + 5% H_2).

The experimental results at temperatures ranging between 600 and 700 °C permitted us to exclude, according to Blasse, the formation of $La_2Li_{0.5}Fe_{0.5}O_4$. Indeed, in the powder diffraction patterns of solids of the above composition, the diffraction peaks typical of the K_2NiF_4 structures

---

*The only references in the literature to an iron-containing member of this family concerns an unsuccessful attempt made by Blasse [3]. Other isomorphous phases with $M^{3+} \equiv Co^{3+}$, Ni^{3+}, Cu^{3+}, Mn^{3+}, Al^{3+} are, in contrast, well known [4 - 8].

were missing and instead appeared the peaks of $LaFeO_3$ and La_2O_3 besides other peaks that could not be ascribed to any other known phase in the ternary system. Moreover in the sintered multiphase solids well-formed pale-yellow crystals were present, probably belonging to a new phase.

We thought it interesting to examine the composition and the structure of this new phase, also considering the relative ease of formation of these single crystals.

2. Experimental details

The samples were prepared by a procedure already employed elsewhere [2]. Proper amounts of lanthanum and iron nitrates are dissolved in water to which is added a small amount of tartaric acid (about 10 wt.%). After heating at about 100 °C, gaseous products are evolved (NO_x, CO_2 and H_2O) causing the viscous liquid to transform into a solid and foamy mass. This solid is then heated in air at 600 °C (1 h) in order to remove the last traces of NO_x and CO_2. X-ray diffraction (XRD) confirms that at such a temperature poorly crystallized $LaFeO_3$ and La_2O_3 already originate. A proper quantity of LiOH is added to the admixture of the two phases, which is then homogenized in an agate mortar, pressed into tablets (500 kg cm^{-2}) and finally heated in a silver vessel in a flowing atmosphere of Ar and 5% H_2 at temperatures between 600 and 700 °C.

The results of the XRD analysis on the samples obtained with the above procedure with a starting composition $La_2Li_{0.5}Fe_{0.5}O_4$ (containing, as already said, $LaFeO_3$, La_2O_3 and the new phase) convinced us that the lithium content of the new phase should be higher than that shown by the starting composition. We prepared therefore a first series of samples having [La]/[Fe] = 4 and [Li]/([La] + [Fe]) ranging from 0.2 to 2.

The XRD analysis of this series clearly showed that the intensities of the reflections of the new phase progressively increased with the lithium content and, when the [Li]/([La] + [Fe]) ratio approached unity, the reflections from La_2O_3 and $LaFeO_3$ were no more noticeable. Finally in samples sintered with an [Li]/([La] + [Fe]) ratio higher than 1.2, reflections from Li_2O appeared beside those of the new phase.

The existence of the biphasic equilibrium between lithium oxide and the new phase facilitated further investigations on the ratio [La]/[Fe] in the composition of the phase and of its possible range. For this purpose we prepared a new series of samples with [Li]/([La] + [Fe]) = 1.5 and [La]/[Fe] from 3 to 5. The results showed that a small variation (±0.1%) in the [La]/[Fe] ratio around 4 caused the reflections or other phases (Li_5FeO_4, $LaLiO_2$) to appear, as well as those of Li_2O and the new phase.

We obtained monophasic samples, by washing with anhydrous methanol the biphasic solids containing the new phase and lithium oxide. These samples, further checked by XRD, were analysed by flame atomic absorption spectrometry for lithium and iron content (Perkin–Elmer 5000).

The iron oxidation number was determined both by permanganometric and by iodimetric analysis which confirmed the presence of Fe^{3+} only. The lanthanum content was assumed equal to that of the starting composition. The powder XRD intensities are collected in Table 1.

Accounting for the experimental data mentioned above, we could confidently assign the composition $LaLi_{0.92}Fe_{0.25}O_{2.33}$ to the new phase.

In the preparation of single crystals for the structure determination we used the technique already successfully employed to obtain the micro-crystalline samples, with only minor variations. The mixture of lanthanum and lithium oxide ([La]/[Fe] = 4) was added to a great excess of lithium hydroxide, carefully homogenized and heated in a silver vessel in flowing

TABLE 1

XRD powder data (Cu Kα)

h	k	l	$d_{(hkl)}$ (Å)	I/I_0
1	1	0	9.362	35
0	0	1	7.497	5
2	0	0	6.620	15
2	1	0	5.921	2
2	2	0	4.681	10
3	1	0	4.186	8
2	2	1	3.971	5
3	2	0	3.672	8
1	1	2	3.480	15
4	0	0	3.310	60
2	0	2	3.261	25
4	1	0	3.211	10
3	3	0	3.121	35
4	0	1	3.028	5
4	1	1	2.952	40
2	2	2	2.926	100
3	1	2	2.792	12
5	1	0	2.596	30
4	0	2	2.481	4
3	3	2	2.398	45
4	4	0	2.341	28
5	3	0	2.271	10
6	0	0	2.206	8
5	1	2	2.134	35
6	2	0	2.093	15
3	2	3	2.066	5
3	6	0	1.974	10
6	0	2	1.901	30
7	1	0	1.872	20
7	2	0	1.818	18
2	0	4	1.803	5
7	3	0	1.738	17
7	1	2	1.675	28

Ar + 5% H_2 for about 10 h at 600 °C. The excess lithium hydroxide slowly decomposes according to the reaction

$$2LiOH \longrightarrow Li_2O + H_2O_{(vap)}$$
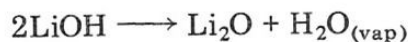
In the earlier stages of the thermal treatment, the LiOH supplied, at the same time, the flux for the crystal growth (melting point of LiOH = 447 °C). The obtained solid mass was washed with anhydrous methanol in order to remove the excess lithium oxide. After preparation of single crystals, whose dimensions ranged from 0.1 to 0.4 mm, their picnometric density was determined in toluene ($\rho = 5.92$ g cm^{-3}).

3. Data collection and structure solution

A suitable crystal of dimension $0.05 \times 0.07 \times 0.15$ mm was selected and analysed on an Enraf–Nonius CAD4 diffractometer using Mo Kα graphite-monochromatized radiation ($\lambda = 0.71069$ Å). The unit cell lattices were determined by least-squares refinements of the setting angles of 25 well centered reflections ($8° < \theta < 25°$). The obtained values were consistent with a tetragonal cell: $a = 13.240(3)$ Å, $c = 7.497(3)$ Å. Diffraction intensities were measured at room temperature in the range $2.5° < \theta < 40°$ by the $\omega/2\theta$ scan method (scan interval 0.9° to 1.2°), with a pre-scan speed of of 16° min^{-1} and a pre-scan acceptance $\sigma(I)/I \leqslant 0.5$. Reflections which did not match the acceptance condition were considered weak; the others were measured at a desired $\sigma(I)/I = 0.005$ for a maximum time of 150 s. Three standard reflections monitored periodically gave no evidence of decay. 2471 intensity data were collected in the octant $+h$, $+k$, $+l$, those with $I > 2\sigma(I)$ were considered as observed. 1456 unique reflections were used in the structure solution and refinement.

The presence of reflections $h00$ and $h0l$ only when $h = 2n$ indicates a Laue class $4/mmm$. Three are the possible space groups but we obtained a good agreement only for the centrosymmetric space group $P4/mbm$ (number 127).

The lanthanum and Fe(1) atoms were located from the super-sharp Patterson map employing the *SHELX-86* package. For all subsequent computations the *SHELX-76* package of crystallographic programs was used. Least-squares and difference Fourier map cycles enabled the location of Fe(2), oxygen and finally lithium atoms.

Refinement proceeded by block diagonal least-squares methods using, in the last cycles, anisotropic temperature factors for lanthanum, iron and oxygen atoms. An empirical absorption correction was applied using the method of Walker and Stuart [4].

The presence of lithium in the iron locations was expected from the lowering of the apparent site occupancy factors for iron in the substitutional sites. The final occupancy factors were obtained after pairs of refining cycles in which alternately the thermal parameters and the occupancy factors

were fixed. The refinement of the structure of $La_{24}Fe_6Li_{22}O_{56}$ shows that a substitution occurs between Fe(1) and Li(4) but gave no evidence of replacement of the Fe(2) and lanthanum atoms.

At convergence, the reliability factor R for the coordinates shown in Table 1 was

$$R = \Sigma|\Delta F|/\Sigma|F_0| = 0.024$$

$$R_w = \{\Sigma\omega|\Delta F|^2/\Sigma\omega|F_0|^2\}^{1/2} = 0.020$$

where $\omega = \sigma^{-2}(F_0)$ and $|\Delta F| = ||F_0| - |F_c||$

4. Structure description

The locations of the lanthanum, lithium, iron and oxygen atoms on the different independent positions of the space group $P4/mbm$ are listed in Table 2*. The resulting formula per unit cell ($La_{24}Fe_6Li_{22}O_{56}$) confirms the experimental values of the chemical analysis for iron and lithium, for iron oxidation number (3+) and for picnometric density (theoretical, 5.96; experimental, 5.92).

In this rather complex structure, iron is always octahedrally coordinated by oxygen: Fe(1) binds four equatorial O(6) and two axial O(5),

TABLE 2

Fractional atomic coordinates and thermal parameters ($Å^2$)

Occupancy	x/a	y/b	z/c	U_{iso} or U_{eq}
16 La 1	0.00799(2)	0.19969(2)	0.25563(5)	0.0062(1)
4 La 2	0.26052(3)	0.76052(3)	0.00000	0.0034(2)
4 La 3	0.21981(3)	0.71981(3)	0.50000	0.0034(2)
0.5 Li + 1.5 Fe 1	0.00000	0.00000	0.00000	0.0094(11)
4 Fe 2	0.08586(9)	0.58586(9)	0.00000	0.0042(5)
4 O 1	0.0000	0.5000	0.1849(10)	0.005(2)
8 O 2	0.03823(5)	0.3773(5)	0.5000	0.011(3)
8 O 3	0.3168(3)	0.8168(3)	0.7102(8)	0.014(2)
8 O 4	0.3212(4)	0.0173(5)	0.5000	0.008(3)
4 O 5	0.0000	0.0000	0.2513(15)	0.009(2)
8 O 6	0.1224(5)	0.1117(5)	0.0000	0.010(3)
8 O 7	0.0303(4)	0.3123(4)	0.0000	0.006(2)
8 O 8	0.1583(3)	0.6583(3)	0.8047(9)	0.013(2)
0.5 Fe + 1.5 Li 1	0.00000	0.00000	0.50000	0.0024(12)
4 Li 2	0.6219(9)	0.1219(9)	0.5000	0.002(3)
8 Li 3	0.981(8)	0.4019(8)	0.1565(22)	0.010(3)
8 Li 4	0.0753(8)	0.5753(8)	0.6499(22)	0.008(3)

*The structural data have been deposited at the FIZ (Karlsruhe).

while Fe(2) binds two O(1), two O(7) and two O(8), as shown in Fig. 1. Li(1) is also octahedrally coordinated by four equatorial O(2) and two axial O(5). Both Fe(1) and Li(1) octahedra are somewhat compressed along the axial (z) direction (c/a ratio = 0.86 for Fe(1) and 0.86 for Li(1) (see Table 3).

Li(3) binds two O(7), one O(1) and one O(3) forming an irregular tetrahedron; similarly Li(4) binds two O(4), one O(1) and one O(8) also in the form of an irregular tetrahedron. Li(2) shows a nearly square planar coordination with two O(3) and two O(4) on opposite corners. Among the three different lanthanum positions (Fig. 2), two (La(2) and La(3)) are coordinated to oxygen in the form of an octahedron. La(2) binds two O(3), two O(6) and two O(8) while La(3) binds the other two O(3), two O(8) and two O(8) and two O(2) with distances ranging from 2.41 to 2.55 Å. Another two O(7) are nevertheless still bound to La(2), but at a distance of 2.853 Å. They are approximately centered on two of the triangular faces of the octahedron forming a pentagonal planar arrangement with the other two O(6) and La(2). In a similar fashion the other two O(4) still bind La(3) at distances of 2.735 Å.

La(1) has a ninefold coordination polyhedron. It might be described as a tricapped triangular prism*. The two bases are formed by O(6), O(6), O(7) and O(2), O(2), O(4) respectively, while O(5), O(3) and O(8) are
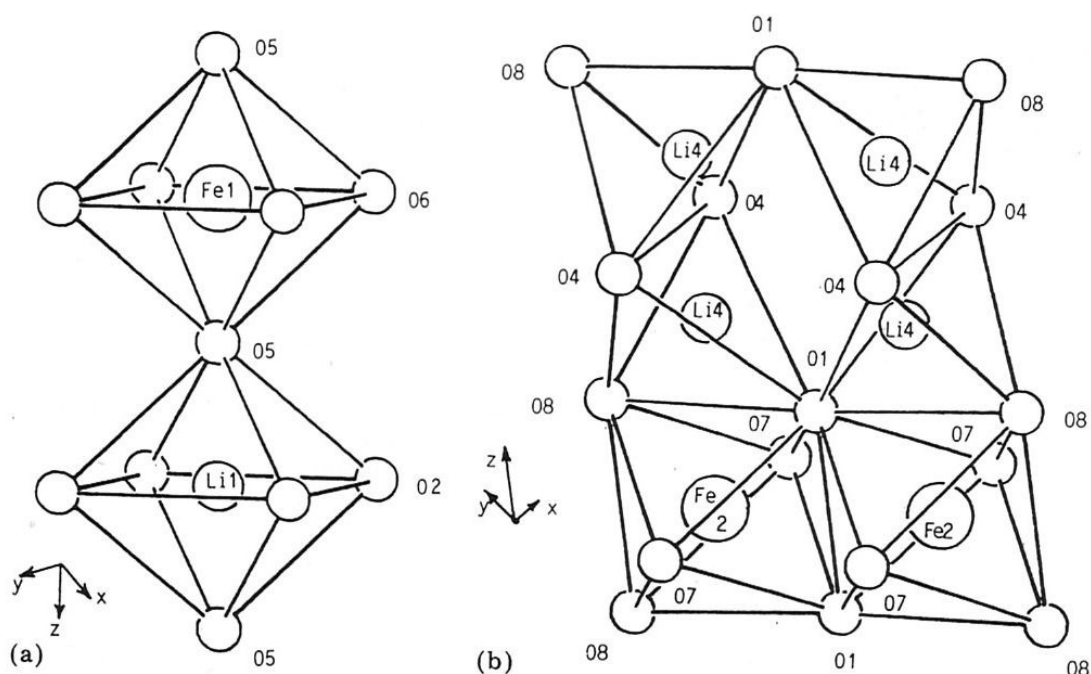

Fig. 1. A chain and (b) B chain.

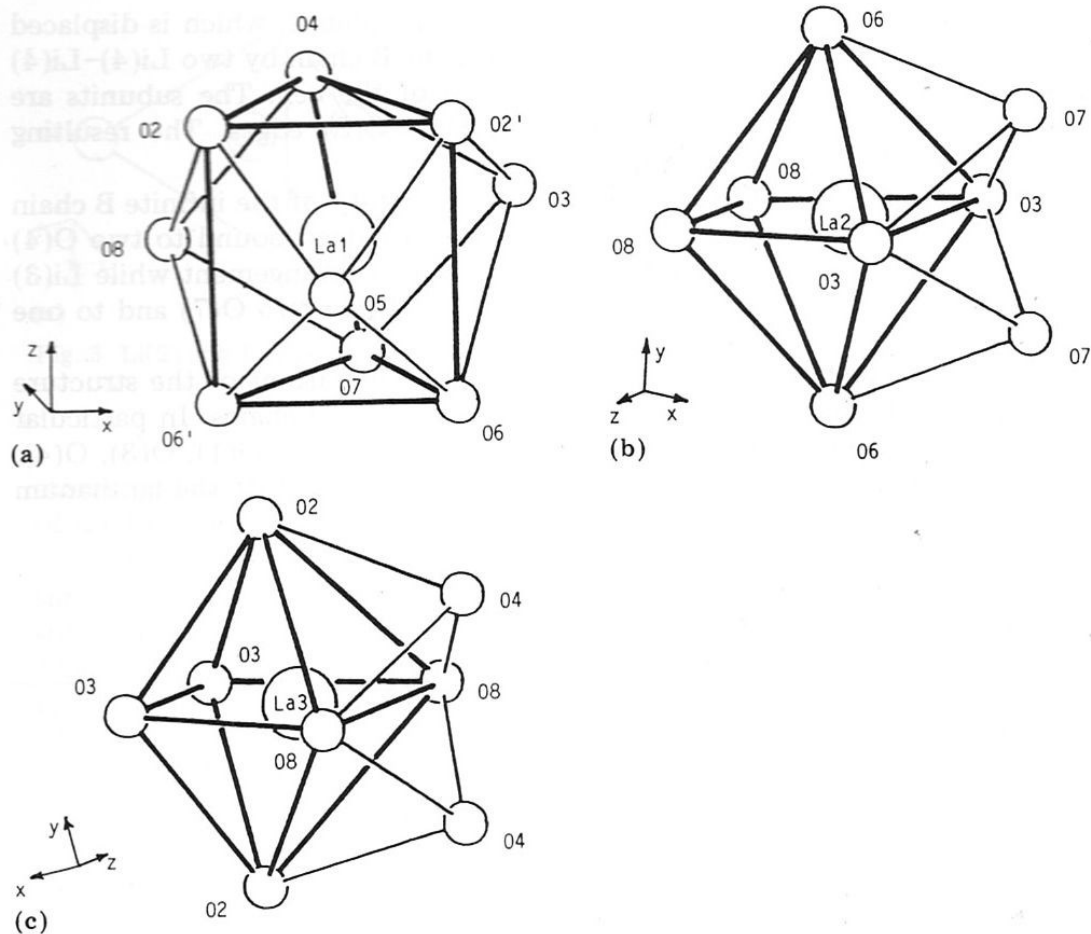*This type of coordination is far from unusual among lanthanides.

Fig. 2. Lanthanum coordination polyhedra.

centered on the three rectangular faces of the prism. The distances range from 2.446 Å to 2.930 Å. It is interesting to note that the prism stretches along z and has a height of exactly $\frac{1}{2}c_0$.

A structural network results from the connection of the described coordination polyhedra: indeed two different types of infinite chain can be seen. They stretch along the z direction, and are both formed by lithium and iron polyhedra.

The first chain, the A chain, originates from the corners of the base of the unit cell as well as from its center for symmetry reasons. The second, the B chain, extends along the middle of each of the side faces of the unit cell. Both A and B chains are repeated twice in every unit cell.

The A chain is obtained through the interconnection of Fe(1) and Li(1) octahedra, by sharing the two O(5) opposite corners; while the B chain is obtained by means of the interconnection of two subunits. The first is formed by two Fe(2) octahedra coupled via the common O(1)–O(1) edge and the second results from the linking of two Li(4) tetrahedra via

the common O(4)–O(4) edge. One Fe(2)–Fe(2) subunit, which is displaced along an equatorial plane, is alternated along the B chain by two Li(4)–Li(4) subunits, which are aligned along the z axis of the cell. The subunits are interconnected by sharing the common O(1)–O(8) edges. The resulting repetitive units are shown schematically in Fig. 1.

Li(2), Li(3) and O(3) are located in the vicinity of the infinite B chain and complement its structure (Fig. 3). Li(2) is indeed bound to two O(4) of the B chain and to two O(3) in a nearly planar arrangement while Li(3) is tetrahedrally bound to one of the above O(3), to two O(7) and to one O(1).

It is worthwhile to notice that all the oxygen atoms of the structure are assigned in the above description either to A or B chains. In particular O(2), O(6) and O(5) are allotted to the A chain, while O(1), O(3), O(4), O(7) and O(8) are allotted to the B chain. It follows that the lanthanum

TABLE 3

Interatomic distances (Å)

| La1	O2		2.677(2)
La1	O2′		2.616(3)
La1	O3		2.802(2)
La1	O4		2.461(1)
La1	O5		2.646(3)
La1	O6		2.706(2)
La1	O6′		2.690(5)
La1	O7		2.446(3)
La1	O8		2.930(4)
La2	O3	(×2)	2.415(2)
La2	O6	(×2)	2.507(3)
La2	O7′	(×2)	2.853(2)
La2	O8	(×2)	2.409(3)
La3	O2	(×2)	2.485(3)
La3	O3	(×2)	2.405(2)
La3	O4	(×2)	2.735(4)
La3	O8	(×2)	2.558(6)
Fe1	O5	(×2)	1.884(2)
Fe1	O6	(×4)	2.194(3)
Fe2	O1	(×2)	2.124(5)
Fe2	O7	(×2)	2.045(4)
Fe2	O8	(×2)	1.995(3)
Li1	O2	(×4)	2.251(3)
Li1	O5	(×2)	1.865(1)
Li2	O3	(×2)	1.950(2)
Li2	O4	(×2)	1.991(3)
Li3	O1		1.849(1)
Li3	O3		1.881(3)
Li3	O7	(×2)	1.895(2)
Li4	O1		1.875(2)
Li4	O4	(×2)	1.932(2)
Li4	O8		1.941(3)
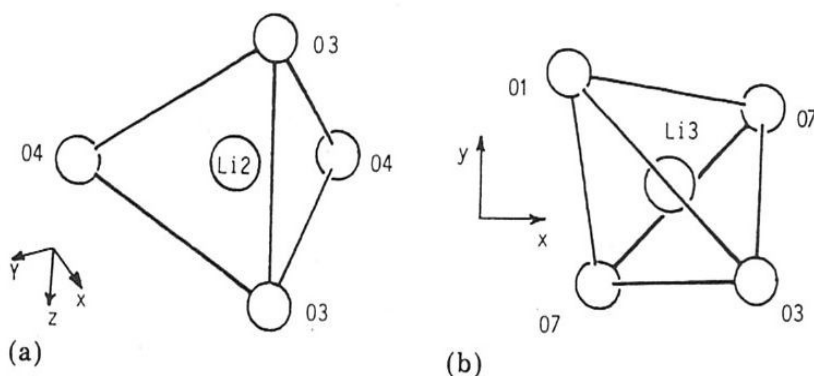
Fig. 3. Li(2) and Li(3) coordination polyhedra.

atoms will be bound exclusively to the oxygen atoms already forming one of the two infinite chains.

From the preceding structure description one can see some marked similarity in the cation environments. Particularly, Fe(1) and Li(1) both show octahedral coordination with similar cation–oxygen distances. Therefore, in the last refinements, a mutual substitution of iron and lithium in Fe(1) and Li(1) sites was assumed. At convergence it was found that some (25% ± 0.3%) of the iron was substituted for lithium in Li(1) and that a corresponding fraction of the lithium was substituted for iron in Fe(1) sites. The R_w value decreased to 2.00%. When similar substitutions were tried between other possible Fe–Li pairs, the results were negative.

It can therefore be concluded that only inside the A chain does an exchange between iron and lithium on the respective positions appear possible. As a consequence, a disruption of the regular sequence –Li–Fe–Li–Fe– takes place, for example with the insertion of some inverted Fe–Li pairs, with a frequency of about 25%, as derived from the refined occupation factors for Fe(1) and Li(1).

References

1 F. Abbattista, M. Vallino, D. Mazza and A. Delunas, *Mater. Res. Bull.*, *20* (1985) 393.
2 D. Mazza, F. Abbattista, M. Vallino and G. Ivaldi, *J. Less-Common Met.*, *106* (1985) 277.
3 G. Blasse, *J. Inorg. Nucl. Chem.*, 27 (1965) 2683.
4 G. Demazeau *et al.*, *Mater Res. Bull.*, *15* (1980) 451.
5 G. Demazeau *et al.*, *Mater. Res. Bull.*, *16* (1981) 47.
6 G. Demazeau *et al.*, *Mater. Res. Bull.*, *7* (1972) 913.
7 F. Abbattista and M. Vallino, *Atti Accad. Sci. Torino*, *116* (1982) 89.
8 F. Abbattista, M. Vallino and D. Mazza, *Inorganica Chimica Acta*, *140* (1987) 147.